RADAR MEASUREMENT OF SURFACE WATER CONTENT DYNAMICS UNDER WHEAT CANOPY

Guy Serbin[1], *Dani Or*[2], and *V. Philip Rasmussen*[1]
[1]Department of Plants, Soils and Biometeorology, Utah State University, Logan, UT, 84322-4820
[2] Department of Civil and Environmental Engineering, University of Connecticut, 261 Glenbrook Road, Unit 2037, Storrs, CT 06269-2037

Abstract— Ground penetrating radar (GPR) with a suspended 1 GHz horn antenna was deployed for measurement of soil water contents and dwarf wheat canopy reflections over bare and electrically terminating surfaces. Surface reflection (SR) magnitudes and propagation times (PT) were used to independently calculate bulk soil dielectric constant and soil water contents.

Measurements over wheat canopy shows that while SR and reflection coefficient values were strongly altered by canopy biomass, PT measurements remain unaffected. Wheat canopy influence on SR gradually intensified during the growth season until the canopy was removed and SR-based measurements rejoined with PT data. Horn-antenna radar measurements over natural surfaces offer a promise for remote truthing of radar data collected from air- and spaceborne platforms, and they may be used in the field for water content and vegetation biomass measurements.

Introduction

Large tracts of the Earth's surface are covered by vegetation. As soil water content and plant biomass are important parameters for climate modeling, agriculture and flood monitoring, remote measurement of these parameters offers promise for wide scale mapping [1].

Traditional methods of radar remote sensing employ frequency domain measurement, with the radar signatures of the aboveground vegetation canopy, soil surface and subsurface all reduced to a single value. Vegetation scattering models developed in recent years are either too simplistic, treating the canopy as if it were a water cloud [2] or utilizing complicated radiative transfer modeling [1, 3] which require extensive ground truthing of numerous biophysical parameters thereby limiting their applicability for routine use.

Ground penetrating radar (GPR) has been employed in recent years for measurement of subsurface and surface water contents, and measurements from vegetation canopy [4-7].

Serbin and Or [6, 7] showed that GPR utilizing a suspended horn antenna allowed for water content estimations via both surface reflection magnitude (SR) and propagation time (PT) measurements. Serbin and Or [7] further showed that SR measurements were influenced by biomass.

The aims of this research were (1) to study the effects of vegetation canopy on subsurface water content measurements, and (2) to see how plant canopies development may be studied via GPR with suspended horn antenna.

Theoretical considerations

Soil dielectric properties

The dielectric properties of soils in the microwave region are functions of volumetric water content [8] frequency [9, 10], mineralogy [11], particle size, shape and orientation to the imposed EM field [12] surface area, bulk density, temperature, and salt content. The dielectric constants of soil solid and gaseous phases are assumed to remain constant with frequency for the entire microwave region.

The most dynamic factor in soils is the water content, that greatly influences the dielectric constant of wet soils due to the large difference between the dielectric constant of water ε_r=81 and that of soil solids ε_r=3~8. The soil water may be decomposed into free and bound water, where bound water refers to the first two molecular water layers to bound solid surfaces that are rotationally hindered by surface forces [13]. Bound water typically has dielectric a dielectric constant around 6 and 30 for the first and second molecular layers, respectively, and is temperature dependent [8, 13-16].

Conversion of measured bulk dielectric constant of soils to water content is often based on the Topp et al. [17] relationships and organic soils utilizing relations by Schaap et al. [18] and da Silva et al. [19].

Reflection of electromagnetic radiation at dielectric boundaries

Incident EM waves reflect at the boundary between two media with differing dielectric properties. The magnitude of the reflection and subsequent transmission of the wave into the second medium are dependent upon the intrinsic impedances of the two media [20]. The reflection coefficient Γ for normal

incidence at a dielectric interface may be expressed as [20]:

$$\Gamma_0 = \frac{E^r_{0,n}}{E^i_{0,n}} = \frac{\sqrt{\varepsilon_n} - \sqrt{\varepsilon_{n+1}}}{\sqrt{\varepsilon_n} + \sqrt{\varepsilon_{n+1}}} \quad (1)$$

where $E^i_{0,n}$ and $E^r_{0,n}$ denote the incident and reflected electric field amplitudes, respectively, *0* denotes normal incidence, ε denotes the relative dielectric permittivity and *n* is an integer denoting the medium.

Acquisition of soil dielectric properties via GPR

GPR units provide time domain reflectivity measurements that are analogous to that of commonly used in-situ time domain reflectometry (TDR) techniques. However, unlike TDR, both the surface reflectivity and the propagation time between reflections can be used to determine soil dielectric properties. A GPR waveform may be viewed in Figure 1 from a dwarf wheat canopy measurement, with antenna, canopy, surface and subsurface reflections clearly annotated. It should be pointed out that these canopy reflections are much smaller than the antenna, surface or subsurface reflections.

Figure 1. GPR waveform from a wheat canopy overlying a wet soil. Physical boundaries are denoted by dash-dot lines, diffuse boundaries between antenna air and air-soil are shown by dashed lines. V_{ant} and V_{surf} denote antenna and surface voltages; t_p denotes propagation time in soil. Canopy reflections are shown as small aboveground reflections in air region.

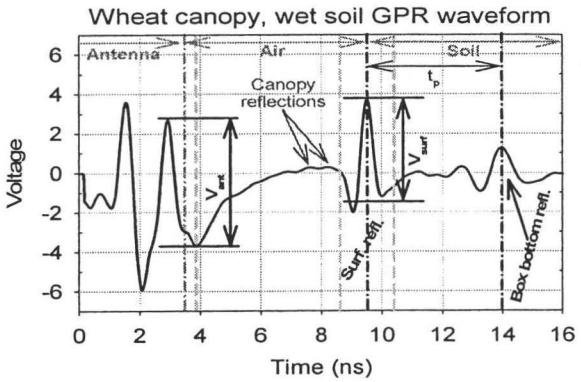

Dielectric properties via surface reflectivity

Surface reflection (SR) measurements utilize the voltage magnitude of the surface reflection, V_{surf}, relative to that of a perfectly reflective (i.e. metal, or "flat plate") surface, V_{fmp}, to determine the surface's reflection coefficient, $\Gamma(t)$, and corrected for temperature induced changes in antenna impedance and height:

$$\Gamma(t) = -\frac{V_{surf}}{V_{fmp}} \cdot ACF \cdot DCF = -\frac{V_{surf}}{V_{fmp}} \cdot \frac{V_{ant,fmp}}{V_{ant}} \cdot \frac{x_{meas}}{x_{fmp}} \quad (2)$$

where *ACF* and *DCF* denote the antenna impedance and antenna-surface distance correction factors, respectively, and the *fmp* and *meas* subscripts of *x* denote the flat metal plate and measurement antenna-surface distances, respectively. The *ACF* is the ratio of the flat plate calibration antenna voltage to that of the voltage of the waveform of interest, and the *DCF* the ratio of the distance between the end of the antenna and the surface to that of the flat plate calibration. Flat plate measurements were acquired at the end of an experiment by covering the soil surface with thick aluminum foil and then acquiring a series of waveforms. The reflection coefficient may the be used to determine ε_b at normal incidence via [20]:

$$\varepsilon_b = \left(-\frac{\Gamma(t) - 1}{\Gamma(t) + 1} \right)^2 \quad (3)$$

and the volumetric water content as a function of ε_b may then be determined via the Topp et al. [17], Schaap et al. [18] or the da Silva et al. [19] relationships, depending on soil composition.

Dielectric properties via propagation time

Radar PT measurement of soil water content is possible when a subsurface reflection exists at a known depth, such as an interface between two different soil types (i.e. sand overlying a silt loam) or between a soil and a metal (silt-loam overlying a layer of aluminum foil). If the distance between two reflections is known, then the two-ways propagation time between them t_p can be used to calculate ε_b via [17]:

$$\varepsilon_b = \sqrt{\frac{ct_p}{2L}} \quad (4)$$

where c is the speed of light in a vacuum ($\sim 3 \cdot 10^8$ m/s) and L is the thickness of the medium (m).

Frequency content of GPR signals

GPR systems utilize ultra-wideband signals that are composed of a wide range of frequencies, with the greatest signal contribution being supplied at the center frequency. Since different media interfaces have differing scattering, transmissive and reflective properties [20], the frequency content of the signal will change as it moved through the media. It was thus found that the time difference between the two

minima of a surface or subsurface reflection could be used to estimate the center frequency, f_c, of a given reflection (as can be seen in Figure 1), via:

$$f_c = \left| \frac{1}{t_{\min 2} - t_{\min 1}} \right| \quad \text{[GHz]} \quad \textbf{(5)}$$

where t_{min1} and t_{min2} denote the times of the first and second reflection minima in ns.

Radar studies of vegetation canopy

As many soils are usually covered by some form of vegetation, the type and state of vegetation cover affects radar backscatter. Significant amounts of research involving the backscatter of vegetation canopy and modeling of such have been done on a variety of vegetation from desert plants to forested areas [1, 2, 21-23].

A number of models have been used for agricultural crops, among them the water cloud model [2], Lang and Sidhu [21] model, radiative transfer models such as the Michigan microwave canopy scattering model [1], and the Karam et al. [22] models and the Stiles and Sarabandi [23] fully phase-coherent scattering model for grasslands.

Vegetation scattering was shown to increase with frequency, such that the lower the frequency the greater the penetration into a canopy [1, 2].

Materials and methods

Ground penetrating radar setup, data acquisition and ground truthing

Remote measurements of the soil surface utilized a Penetradar IRIS-L GPR unit and a 30 AGC monostatic horn antenna (Penetradar Corp., Niagara Falls, NY) that utilizes a monocycle signal with a center frequency of 1.0 GHz and a pulse width of 1 ns.

The horn antenna irradiates an elliptical pattern on the soil surface with an area that varies with height from above. The majority of the radiation is concentrated in the center of the ellipse and the electric field is polarized with the minor (y) axis of the ellipse towards the front end of the antenna. The irradiation ellipse radii were determined using linear regression:

$x(z) = 0.332\,z + 0.1048$ [m] **(6a)**

$y(z) = 0.1557\,z + 0.0821$ [m] **(6b)**

where $x(z)$ and $y(z)$ denote the major and minor radii as a function of height z in meters. Rotation of the antenna on the x-axis to an oblique angle will result in *horizontal polarization* and along the y-axis in *vertical polarization*. It should be noted that as the height of the antenna is increased above the ground surface, the intensity of the measured surface reflection decreases due to air spreading losses [20].

The reflected radar pulse differs from the initially generated monocycle signal, and consists of a central maximum with two voltage minima on either side, with a time of about 1 ns between these two voltage minima. Positive reflections, such as the air- soil surface reflection, will occur at interfaces where the underlying $\varepsilon_{n+1} > \varepsilon_n$. In cases where the pulse propagates from a medium of greater ε to that of a lesser one (such as a subsurface void or the surface-air reflection that is sometimes seen off a returning wave from a strong subsurface reflector), a negative reflection can be seen.

The acquired GPR waveforms are 1600 data points (40 ns) in length, with the initial data points ideally occurring in or before the antenna. The system was monitored to eliminate waveform drifting.

Greenhouse studies

The radar unit was deployed in a greenhouse to measure soil water drying patterns during growing season of wheat canopy. The dwarf wheat cultivar planted was USU 9-2-2 that was developed at the USU Crop Physiology Lab with maximal canopy height of 0.4 m to facilitate antenna placement at 1 m above the soil surface while measuring through a "uniform" canopy.

Wheat was planted in two 1.44 m^2 square planters on a 2.5 cm square grid. The planters had wheels on the bottom which allowed them to move along a track on the ground underneath the antenna, which was fixed in place. One planter utilized a bare soil surface, and the other had the surface covered with electrically terminating aluminum foil (i.e. surface that theoretically would have the same reflective properties), hereforth referred to as the "unterminated" and "terminated" boxes, respectively. Each planter was filled with peat-perlite artificial soil mixture (bulk density of about 140 kg/m^3) to a depth of 0.14 m, above a 1 cm thick layer of gravel. The bottom of each planter was terminated with aluminum foil to reflect radiation and mark the location of the bottom for PT measurements. Holes were drilled through the aluminum foil bottom to allow for adequate drainiage and aeration of the root zone. After planting the soil surface settled to a total thickness (including gravel) of about 12 cm.

Because of the setup used in the greenhouse, concurrent measurements from terminated and unterminated boxes were not possible, as each box had to be manually moved underneath the antenna for measurements.

Ground truthing of water content in the unterminated plot utilized a 15 cm long 3-rod TDR

Figure 2. Representative diagram of wheat measurements.

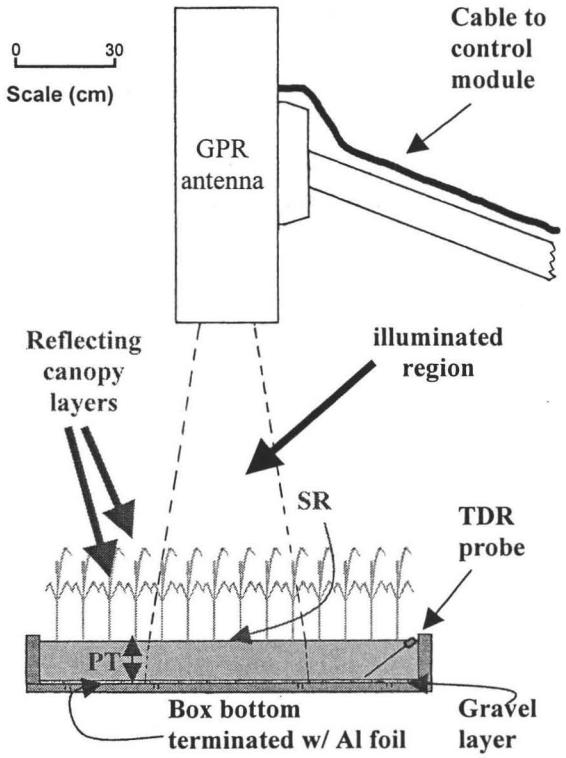

probe was placed diagonally at the edge of the box while the canopy was growing, and gravimetric measurements in the absence of canopy. A representative diagram of the setup may be seen in Figure 2.

The terminated plot had seeds planted in short straws to ensure that the meristems would germinate upwards and not underneath the aluminum foil (which covered 92% of the surface), with the straws being removed once the wheat had germinated and shoot could be seen above them.

The wheat was planted on March 9, 2002, and GPR canopy measurements of the unterminated box were acquired every 30 minutes starting on March 15, 2002. For the first few weeks water was applied by spraying to prevent damage to wheat plants, followed by flood irrigation for the remainder of the season. Canopy height was monitored every few days using a tape measure. Terminated canopy measurements occurred for two days April 11 to 13, 2002, and then with single measurements occurring once every few days thereafter. On May 7, 2002 the canopies were removed and biophysical parameters such as number of tillers, tiller lengths and tiller section lengths, number of leaves and leaf areas were measured. The bare soil in the unterminated box was re-irrigated the next day and the drying curve was measured until May 21, 2002. Measurements from the non-canopy covered terminated box were also collected, as well as flat plate calibrations from both boxes. Soil water content was ground truthed via TDR during canopy development, but after canopy removal gravimetric measurements were also acquired.

Soil water contents were derived from measured bulk dielectric properties via the da Silva et al. [19] relationships for a peat-perlite mixture:

$$\Theta_v = -0.1430 + 0.1203\sqrt{\varepsilon_b} \quad [\mathrm{m^3/m^3}]. \qquad (7)$$

Physiology of dwarf wheat

The USU 9-2-2 dwarf wheat cultivar used had between 3-5 tillers per plant and 4-4.5 leaves on average per plant. Mature plants usually had two leaf layers, where the top layer consisted of flag leaves (the largest and highest leaf of the tiller) and the second layer consisting of normal wheat leaves several cm below it. Seed heads were usually located 1-4 cm above the base of the flag leaves, with 1 seed head per tiller, with these shown in Figure 2.

Results and discussion

Canopy development characteristics between unterminated and terminated boxes

Differences in canopy development were noted between the unterminated and terminated boxes. The terminated canopy was shown to develop faster and higher than the unterminated canopy, and showed a higher leaf area index. Between 17 and 44 days after planting the measured terminated box canopy heights were about 4 cm higher than the unterminated box, after which the canopy heights become similar. Total canopy LAI at canopy removal was 6.9 and 9.7 m^2/m^2 for the unterminated and terminated boxes, respectively, and directly beneath the antenna these values become 4.5 and 12.1 m^2/m^2, respectively.

Unterminated surface measurements

Radar measurements of the unterminated canopy and the underlying soil can be seen in Figure 3, which compares SR and PT from the beginning of canopy measurements to canopy removal, and the subsequent bare soil drying patterns thereafter. Canopy heights can be seen also in this figure. Differences in irrigation patterns can clearly be seen as prior to 25 days after planting the soil was gently sprayed to prevent plant damage, and after this initial period the surface was flood irrigated for a few minutes at each irrigation to produce spatially homogenous water contents. Because of this and the lack of a full canopy (canopy height h_c was below 22 cm) SR measurements were frequently greater than

PT values except during drying. However, once flood irrigation commenced this pattern reversed itself and PT exceeded SR, and as canopy height (and thus biomass) increased, so did the discrepancies between the two. SR measurements show that as canopy height h_c increases, the overall range of SR measured water contents decreases for both maximal and minimal values. For a fully developed canopy SR values are much lower, often by almost 0.2 m^3/m^3, than PT values and the two only approach one another or cross after several days of drying under a transpiring canopy. Unlike previous radar measurements from inorganic soils [7], no evidence of bound water release effects were seen in these measurements, possibly due to the low bulk density of the soil which would have resulted in a low bound water content (even if the specific surface area of the peat-perlite mix was high, the low bulk density would compensate), such that temperature changes would have minimal effects. Also, the presence of a greenhouse affects radiation balance, minimizing diurnal temperature fluctuations.

Figure 3. Water content and canopy height measurements from the unterminated box.

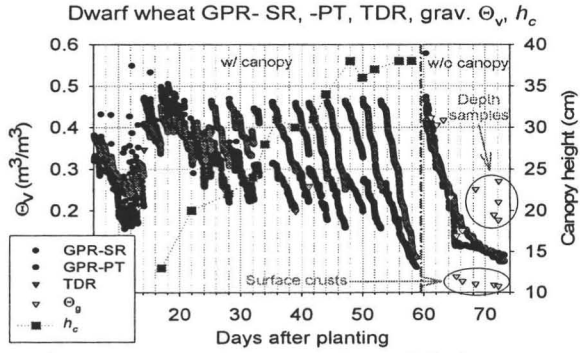

The decrease in SR correlates with an increase in canopy biomass, which served to scatter away radiation and induce canopy reflections, which can be seen in Figures 4A-B. It should be noted that the highest canopy reflection usually occurred 8 cm below the top of the canopy, as canopy height is a measure of the tallest plants in the canopy but not the plant average height or vertical density distribution. Canopy reflections became evident approximately a month after planting; and a week after that another canopy reflection appears beneath it. The top reflection correlates with flag leaves and wheat seed heads (specifically with the average tiller length at the end of the experiment), and the layer beneath that correlates with an underlying leaf layer (Figure 4A), with the intensity of these reflections increasing with time (Figure 4B). Vegetation canopy reflections were not visible prior to one month due to the size and magnitude of the surface refection (on the order of several volts), which would have masked canopy reflections (on the order of tenths of a volt).

PT measurements were always higher than SR and were unaffected by canopy cover as the measurement was not dependent upon reflection amplitude but rather reflection location (travel time). Removal of the canopy resulted in a large increase in SR values, with SR values exceeding or equaling PT values, with SR values appearing to sharply decrease and then level off 4.5 days after irrigation and a constant decrease in PT (the sharp decrease is also echoed in the PT as well, though not as greatly). It should be noted that data logger panel temperatures (not shown) showed an increase of 5 to 10°C in maximum

Figures 4A-B. A. Unterminated plot canopy and canopy reflection heights. Top and 2nd denote the flag leaf/ seed head and underlying leaf layer reflections, respectively. B. Leaf layer reflection voltages.

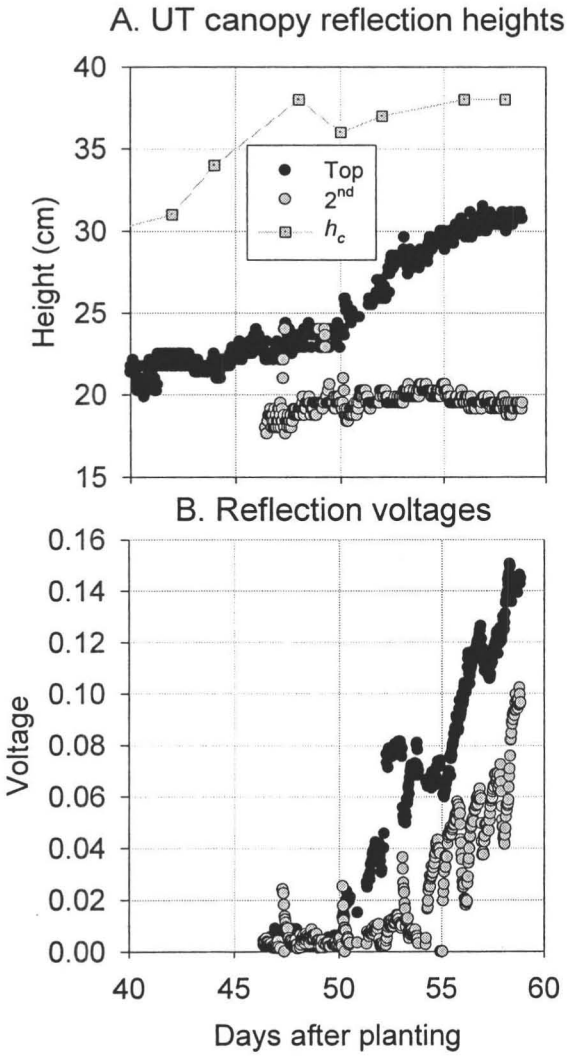

temperatures in the greenhouse relative to days prior to this sudden decrease.

Comparison of SR and PT with gravimetric measurements show that at higher water contents both SR and PT appear to underestimate water content, SR appears to show the closest agreement with gravimetric, with PT showing lower values, particularly when the soil is wet or conversely very dry. Potential explanations for this would either be due to the dryness and low bulk density of the top surface layer (which approached a few hundredths of a m^3/m^3 in advanced stages of drying), which would cause a region of very low permittivity (similar to air) and thus cause the radar to sample at a greater depth. This would then effectively lower the effective distance of the travel path L and thus bias PT measurements such that the measured propagation time/distance would be less than should be and underestimate water content. Errors in measurement of L could have also biased PT- any error on the order of a few millimeters could bias measurements by a few percent or more.

Figure 5. Absolute value of reflection coefficient and canopy height measurements from the terminated box.

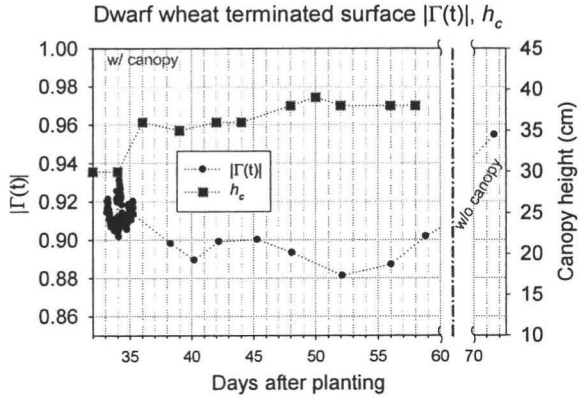

Terminated surface measurements

Measurements from the terminated surface, as seen in Figure 5, show that as canopy height and thus biomass increase the absolute power of the surface reflection coefficient decreases. These decreases can be seen occurring the most while the canopy height is still increasing, after which values become more or less stable. Removal of the canopy causes a large increase in total reflected energy, showing that a significant amount of energy had indeed been scattered by the canopy above.

Frequency effects of canopy upon the GPR signal

As canopy was found to affect surface reflectivity measurements from both unterminated (Figure 3) and terminated (Figure 5) boxes, an analysis of the surface reflection center frequency was performed to see what information could be gleaned from this, as can be seen in Figures 6A-B.

For the unterminated box (Figure 6A), different behaviors are seen between early and late stages of growth and also between the existence and lack of canopy. Early stages of growth were noted by gentle spraying which was thought to increase the salinity of the soil, which would have increased its reflectivity and attenuation, possibly resulting in low center frequencies for the reflected signal. As the soil dried out the frequency content of the soil was seen to increase. This part of the canopy measurement also seems to have been very noisy, and possibly due to the existence of a low, dense canopy whose reflections may not have been visible yet still added enough noise to effectively widen the subsurface peaks. As the canopy matured, these canopy reflections then became distinct aboveground reflections, and the maximal center frequency was shown to be inversely related to the canopy height and water contents. Removal of the canopy caused a large increase in center frequency to above 1 GHz, but the behavior then reversed itself, with only an initial increase in f_c with drying followed by a

Figures 6A-B. Center frequency values for (A) the unterminated and (B) terminated boxes.

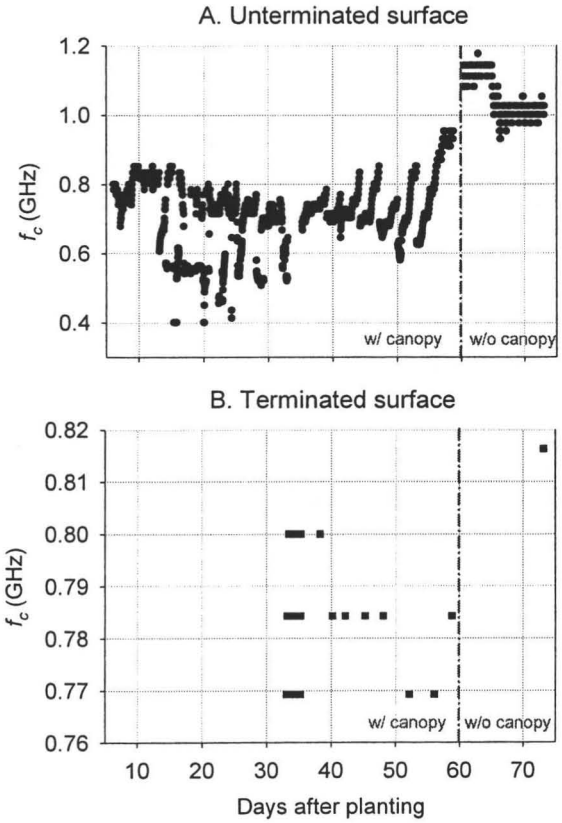

subsequent decrease. It is surmised that due to high temperatures in the greenhouse the surface dried out quickly, allowing the radiation to penetrate deeper into the soil and showing an effective surface at a deeper depth than the actual surface, and scattering away more of the higher frequencies, as shown by SR and PT data as well.

Terminated surface data (Figure 6B) also suggest a decrease in frequency with canopy height, but it appears that the changes are only on the order of 10s of MHz due to the highly reflective nature of the aluminum foil, with the majority of the frequency response occurring at around 785 MHz. Removal of the canopy shows an increase to 815 MHz, indicating that the frequency content was also affected somewhat by the canopy.

Conclusions

Dwarf wheat canopy biomass development affected surface reflection (SR) measurements but did not influence propagation time (PT) data. Dwarf wheat canopy layers induce well-defined reflections corresponding to phonological development above a minimum height (~0.17 m for a 1 GHz antenna) and certain LAI, prior to which canopy reflections were masked by the surface reflection. Ability to discern canopy properties offers a promise for canopy corrective indices and future studies of biomass development with radar.

This technology and setup potentially allows for mapping of subcanopy water contents, near-surface remote truthing of radar data from air- and spaceborne sensors and the study of vegetation canopy cover.

Acknowledgements

We acknowledge Bill Mace for his assistance with field work and construction of the GPR antenna mast and wheat planters. Yaacov Kapiluto, Robert Love, Laureen Kelly, Michael Sukop, Markus Berli, Priscila Palmer and others are gratefully acknowledged for their assistance in planting wheat. Funding for the GPR unit was provided in part by Phil Rasmussen, the United States-Israel Binational Agricultural Research and Development Fund (BARD) through project no. IS-2839-97, and the Utah Agricultural Experimental Station (UAES). The Rocky Mountain Space Grant Consortium is also acknowledged for providing a graduate research fellowship.

References

[1] F. T. Ulaby, P. C. Dubois, and J. van Zyl, "Radar Mapping of Surface Soil Moisture," *Journal of Hydrology*, vol. 184, pp. 57-84, 1996.

[2] M. C. Dobson and F. T. Ulaby, "Preliminary Evaluation of the SIR-B Response to Soil Moisture, Surface Roughness and Crop Canopy Cover," *IEEE Transactions on Geoscience and Remote Sensing*, vol. GE-24, pp. 517-526, 1986b.

[3] M. A. Karam, A. K. Fung, R. H. Lang, and N. S. Chauhan, "A Microwave Scattering Model for Layered Vegetation," *IEEE Transactions on Geoscience and Remote Sensing*, vol. 30, pp. 767-784, 1992.

[4] A. Chanzy, A. Tarussov, A. Judge, and F. Bonn, "Soil Water Content Determination Using a Digital Ground-Penetrating Radar," *Soil Science Society of America Journal*, vol. 60, pp. 1318-1326, 1996.

[5] J. A. Huisman, C. Sperl, W. Bouten, and J. M. Verstraten, "Soil water content measurements at different scales: accuracy of time domain reflectometry and ground-penetrating radar," *Journal of Hydrology*, vol. 245, pp. 48-58, 2001.

[6] G. Serbin and D. Or, "Diurnal Measurements of Near-Surface Water Content Using Ground Penetrating Radar (GPR)," presented at Rocky Mountain NASA Space Grant Consortium 2002 Fellowship Student Symposium, University of Utah, Salt Lake City, UT, 2002.

[7] G. Serbin and D. Or, "Near-Surface Soil Water Content Measurements Using Horn Antenna Radar - Methodology And Overview," *Vadose Zone Journal*, pp.?-?, 2003?

[8] D. Or and J. M. Wraith, "Temperature effects on soil bulk dielectric permittivity measured by time domain reflectometry: A physical model," *Water Resources Research*, vol. 35, pp. 371-383, 1999.

[9] P. Debye, *Polar Molecules*. Dover, Mineola, N.Y., 1929.

[10] J. B. Hasted, *Aqueous Dielectrics*. London: Chapman and Hall, 1973.

[11] A. von Hippel, "Dielectric Materials and Applications." Cambridge, MA: The M.I.T. Press, 1954.

[12] S. B. Jones and S. P. Friedman, "Water Content and Particle Shape Effects on the Dielectric Permittivity of Anisotropic Media," presented at Third Workshop on Electromagnetic Wave Interaction with Water and Moist Substances, Athens, Georgia, 1999.

[13] J. O. M. Bockris, E. Gileadi, and K. Muller, "Dielectric Relaxation in the Electric Double Layer," *The Journal of Chemical Physics*, vol. 44, pp. 1445-1456, 1966.

[14] M. C. Dobson, F. T. Ulaby, M. T. Hallikainen, and M. A. El-Rayes, "Microwave Dielectric Behavior of Wet Soil- Part II: Dielectric Mixing Models," *IEEE Transactions on Geoscience and Remote Sensing*, vol. GE-23, pp. 35-46, 1985.

[15] G. Serbin, "Microwave Thermodielectric Behavior of Soil-Water Mixtures and Their Potential Effects on Microwave Remote Sensing," in *Department of Geological and Environmental Sciences*. Beer Sheva, Israel: Ben Gurion University of the Negev, 2001, pp. 138.

[16] S. B. Jones and D. Or, "Surface area, geometrical and configurational effects on permittivity of porous media," *Journal of Non-Crystalline Solids*, vol. 305, pp. 247-254, 2002.

[17] G. C. Topp, J. L. Davis, and A. P. Annan, "Electromagnetic determination of soil water content: Measurements in coaxial transmission lines," *Water Resources Research*, vol. 16, pp. 574-582, 1980.

[18] M. G. Schaap, L. D. Lange, and T. J. Heimovaara, "TDR calibration of organic forest floor media," *Soil Technology*, vol. 11, pp. 205-217, 1997.

[19] F. F. da Silva, R. Wallach, A. Polak, and Y. Chen, "Measuring Water Content of Soil Substitutes with Time-domain Reflectometry (TDR)," *Journal of the American Horticultural Society*, vol. 123, pp. 734-737, 1998.

[20] F. T. Ulaby, *Fundamentals of Applied Electromagnetics*. Upper Saddle River, NJ: Prentice Hall, 1999.

[21] R. H. Lang and J. S. Sidhu, "Electromagnetic Backscattering From a Layer of Vegetation: A Discrete Approach," *IEEE Transactions on Geocience and Remote Sensing*, vol. GE-21, pp. 62-71, 1983.

[22] M. A. Karam, F. Amar, A. K. Fung, E. Mougin, A. Lopes, D. M. Le Vine, and A. Beaudoin, "A Microwave Polarimetric Scattering Model for Forest Canopies Based on Vector Radiative Transfer Theory," *Remote Sensing of Environment*, vol. 53, pp. 16-30, 1995.

[23] J. M. Stiles and K. Sarabandi, "Electromagnetic Scattering from Grassland- Part I. A Fully Phase-Coherent Scattering Model," *IEEE Transactions on Geoscience and Remote Sensing*, vol. 38, pp. 339-348, 2000.